



Concrete deep beam with strut reinforcement

Hussein Kamal Kadhim^a and Mazin Diwan Abdullah^a

^aDepartment Civil Engineering / College of Engineering / Al-Basra University / Al-Basra, Iraq

*Corresponding author E-mail: pgs.hussein.kamal@uobasrah.edu.iq

DOI:10.52113/3/eng/mjet/2023-11-02/47-61

Abstract

The study numerically examined eight concrete deep beam specimens seven with strut and one reference with normal reinforcement the reinforcement quantity varied among the specimens, yet none exceeded the amount present in the reference sample. In instances where an excessive amount of reinforcement was situated in the strut area, it was judiciously redistributed to bolster the reinforcement configuration of the specimens. The specimen tested using abaqus program. Upon examining the results, it was observed that the strut reinforcement technique was more effective than conventional reinforcement, providing an (5% to 10%) increase in maximum load capacity depending on the type of concrete used. Additionally, it resulted in a decrease of (6 to 42%) in the amount of compression reinforcement needed. The study also revealed that having additional reinforcement, such as shear reinforcement or any other reinforcement, in the mid-span of a deep beam and away from the stress zone does not provide any significant benefit, unlike reinforcement in the stress zone, which increases the strength of the beam. It was also noted that cracks are formed in the shear and flexural zones at reference specimen when a load less than the specimens with strut is applied. The displacement in specimens with strut was less than of reference sample. It was also found that strain in specimens with strut reinforcement was lower than in reference specimen.

Keywords: Deep beam, Strut and tie specimen, Reinforcement strut, strain, two points load, Abaqus program.

1. Introduction

Deep beams are structural members characterized by their relatively large depth compared to their span. They are commonly used in various civil engineering applications, such as bridges, transfer girders, and foundation beams. Due to their unique geometry, deep beams experience complex load distributions and stress patterns, requiring specialized design considerations. One of the primary challenges in designing deep beams is their ability to resist shear forces. Unlike regular beams, deep beams are more prone to shear failures due to the increased amount of shear stress developed in their span. Researchers have extensively studied the behavior of deep beams to develop effective design approaches and guidelines. Several failure modes can occur in deep beams, including crushing of strut failure, diagonal-splitting failure, and shear-compression failure. Crushing of strut failure happens when the concrete struts in the deep beam experience excessive compressive stresses, leading to concrete crushing. Diagonal-splitting failure occurs when inclined cracks propagate diagonally across the beam, usually from the loaded area towards the supports, due to shear stresses exceeding the concrete's shear strength. Shear-compression failure involves the crushing or failure of concrete in the compression zone of the deep beam, resulting from high applied shear forces and resultant compressive stresses. Designing deep beams involves considering factors such as the concrete strength, reinforcement detailing, shear reinforcement, and load distribution. Various design codes and guidelines, such as ACI (American Concrete Institute) and Eurocode, provide specifications and procedures for the design of deep beams. These codes incorporate research findings and experimental data to ensure the reliability and efficient design of deep beams in civil engineering structures. Deep beams play a crucial role in structural engineering, particularly in supporting heavy loads and spanning long distances. Understanding the behavior of deep beams and incorporating appropriate design considerations is essential to ensure their structural integrity and safety. Ongoing research and advancements in design methodologies continue to contribute to the development of efficient and reliable deep beam designs. Cheng & Tan [1] three experiments totaling 36 beams were utilized to demonstrate STM's superiority.

This diagonally fractured deep beam (DB) was utilized to construct this connected arch. Without web reinforcing, it has been shown that the shear strength (SS) of a beam decline with member size. This is related to the phenomenon known as the size effect. In this investigation, the strut-and-tie specimen (STM) and the finite element specimen (FEM) are used to examine the relationship between size and the (SS) of (DB). Research indicates that the principal cause of the size effect in concrete beams is the incorrect use of the shear transfer concept originally established for steel beams. Secondary features that may impact overall frame proportions include strut geometry and web reinforcement spacing. Oh & Sin, 2001 [2] was tested fifteen concrete deep beams (DB) with reinforcement subjected to Two-point load with compressive strengths ranging from 23 MPa to 74 MPa to determine their ultimate shear and symmetric diagonal cracking strengths. Both the (a/d) and the (l/d) were shifted from 0.5 to 2.0 and 3.0 to 5.0, respectively. All the beams were reinforced with a single layer, with specific values for the transverse reinforcement (r_t), vertical reinforcement (r_v), and horizontal reinforcement (r_h), which were 0.0129, 0.0034, and 0.0094, respectively. The ultimate shear failure mode of DB was defined by the a/d ratio regardless of the concrete strength. When the a/d was dropped, the DB produced with HSC (High strength concrete) abruptly and unexpectedly collapsed, in contrast to the DB made from regular concrete, which gradually deteriorated. The findings show that the aspect ratio a/d is the most important element in determining the ultimate shear strength of deep beams. When applied to DB with HSC, ACI Code Eq. (11-29) significantly underestimates the significance of both concrete compressive strength (f_c) and longitudinal steel reinforcement r_t (11-30). Adding horizontal shear reinforcement to deep beams constructed of HSC does not improve ultimate shear strength as a function of a/d . The Li Group, (Wen-Yao Lu, 2013) [3] this research reports the results of testing 16 distinct reinforced concrete deep beams. The bearing plates took the brunt of the force in eight of the tests, while the columns did the heavy lifting. The existence of horizontal and vertical stirrups, as well as the processes involved in force transmission, were the primary foci of the investigation. An increase in compressive strength was shown to significantly enhance shear strength, provided the shear span to depth ratios (a/d) of the deep beams were maintained. However, the ratio of horizontal to vertical stirrups determined the extent to which shear strength was increased. The deep beams' crucial flexure sections were found to be the half load-bearing plate's centroid and the load column's sidewalls. By taking into account the processes responsible for force transmission, this research proposes an analytical technique for determining the shear strength of deep beams. Both the ACI 318-08 STM [4] (Strength Theory Specimen) and the suggested technique were compared to existing test results and rated on their ability to forecast shear strength. Shear strength predictions for reinforced concrete deep beams were shown to be more accurate using the suggested approach than using the STM (strut and tie modelling) presented in ACI 318-08. Ning Zhang, Kang-Hai Tan, 2007 [8] conducted an experimental program that included a set of 11 specimens divided into three groups. In most cases, the shear strength of deep beams decreases as their height increases due to the size effect. It is known that after diagonal cracking occurs, deep beams behave differently from shallow beams, with arch action predominating instead of flexure. However, the causes of size-related effects in deep beams are still unknown. It is hypothesized that factors affecting the strength of the compression component, such as vertical reinforcement design and boundary conditions, also influence the size effect. The experimental program provides data to support the hypotheses developed from the strut-and-tie specimen. It has been shown that the size effect on the ultimate shear strength of plain concrete beams with large height-to-width ratios can be mitigated if the loading and support plates are carefully designed. The study also demonstrates that uniformly distributed vertical reinforcement can help reduce the size effect. The study also investigates the influence of nonlinear forces on column strength. The modified strut-and-tie specimen is recommended as a more accurate tool for predicting shear strength, considering the sources of the size effect, compared to other tested techniques. Kamaran Sulaiman Ismail, 2016 [9] as part of an extensive experimental program, the study of 24 concrete deep beam with reinforcement is in progress. Concrete strength, the ratio of a/h , shear reinforcement, and member depth were among the factors studied. To gain a better understanding of the magnitude and distribution of stresses within the shear span, finite element analysis (FEA) using the M4 micro plane specimen in ABAQUS software was employed. This specimen, implemented as a VUMAT code, was validated against experimental tests on concrete deep beam with reinforcement, providing a more accurate representation of concrete behavior. An additional evaluation of the effects of concrete strength, a/d , and shear reinforcement is performed using this specimen in a parametric research. The results of the experiments and the numerical simulations show that the SS depends on the size of the beam and that the concrete strength and a/h are the two most important parameters in determining the behavior of concrete deep beam with reinforcement. In addition, the results show that the parameter of concrete strength varies with size. Adding a small amount of shear reinforcement may boost the shear capacity of concrete deep beam with reinforcement by roughly 20%, but adding more than that does not significantly increase capacity, as shown by the findings of the study. Appa Rao, G 2021 [10] 10 Deep beam (DB) having a/d of 1.0 are experimentally evaluated. Nine out of the ten DB had web reinforcing applied, which increased their load bearing capability by up to 15%. A 0.3-millimeter-wide diagonal fracture was reported at the beam's service load. Both the vertical and horizontal web reinforcement ratios of the beam exceeded 0.46. By reinforcing webs in both directions, we can effectively limit the spread of diagonal cracks. Experimental tests conducted as part of the current study and extensive DB data points gathered from prior research were used to analyze the ACI 318-19 strut and tie specimen (SATM) provisions for DB with web reinforcement. It has been found that ACI 318-19 provides more reliable predictions of DB shear capacities than AASHTO, the average strength ratio is 0.67. The ACI 318-19 SS requirements have been proved to be conservative. Beams that failed for causes other than tie yielding have been used to estimate the ACI 318-19 strut coefficient. Studies have shown that the strut coefficient is very sensitive to the strength of the concrete. Therefore, it is probable that a DB capacity prediction made with a single strut factor will be dangerous. Mona Saleha Mohammad, 2023 [11] Numerical simulations utilizing the Abaqus/standard program are used to examine the behavior of concrete deep beam with reinforcement web apertures in this research. For many different factors, the verified specimens' numerical findings agreed well with the experimental ones. These included the a/d , opening size and placement, main reinforcement ratio, and

web reinforcement ratio. The results showed that the carrying capacity of concrete deep beam with reinforcement is reduced when they have apertures, especially those between 0.3 and 0.4 of the beam's total height. Furthermore, holes cut across the shear zone significantly reduce the maximum pressure, particularly along the loading path and near to the bearing plate. This is because shear cracks tend to congregate in the corners of apertures along the loading path line. Size and location of web openings have a significant impact on the behavior of concrete deep beam with reinforcement. When the a/d is decreased, the ultimate load also rises. Increasing compressive strength increases its ultimate bearing capacity. In a similar vein, increasing the main reinforcement ratio to reduce cracking results in a higher ultimate load. The same conclusion holds true for the bearing capacity of web-opened concrete deep beam with reinforcement when the web reinforcement ratio is considered. In order to improve the bearing capacity of concrete deep beam with reinforcement by 11.36% and 3.26%, respectively, an increase in the main reinforcement ratio from 0.45% to 0.57% and an increase in the web reinforcement ratio from 0.29% to 0.33% are both possible. Chen, Z., & Wang, Y. (2023) [14] the objective of this research was to evaluate the performance of normal strength reinforced concrete deep beams under triangular distributed loading. Experimental tests were conducted on deep beams without any supplementary additives. The findings revealed that the load-carrying capacity and deflection characteristics of the deep beams were influenced by the loading pattern and the shear span-to-depth ratio. The presence of adequate flexural reinforcement contributed to enhanced beam stiffness and resistance to excessive deflection. The study emphasizes the influence of loading pattern and shear span-to-depth ratio on the load-carrying capacity and deflection characteristics of normal strength reinforced concrete deep beams subjected to triangular distributed loading. Zhang, L., & Liu, H. (2023) [15] this study examined the behavior of reinforced concrete deep beams under a combination of concentrated and uniformly distributed loading. Experimental tests were conducted on deep beams made of ordinary concrete without any additional admixtures. The results demonstrated that the load-carrying capacity and crack propagation pattern of the deep beams were affected by the ratio of concentrated to distributed loading, as well as the shear reinforcement ratio. The presence of appropriate shear reinforcement resulted in improved shear resistance and ductility. The investigation underscores the importance of the ratio of concentrated to distributed loading and the shear reinforcement ratio in determining the load-carrying capacity and crack propagation behavior of reinforced concrete deep beams subjected to a combination of concentrated and uniformly distributed loading.

2. Experiential program

2.1. Procedure of work

Eight specimens were used one specimen with normal reinforcement was used as a reference to compare the other specimens with strut reinforcement under two-point load. All of the specimens were made with concrete that has a normal strength (30 MPa). A real-world optimization method is built on top of the specimen that was offered. Deep beams were put through tests to see how these changes changed how well they worked and how they behaved. Figure 1 shows all of the specimen forms. The beam was 1100mm long, 150mm wide, and 400mm high, and the angle between the strut's axis and the tie was 44 degrees. The frame was strong and stable, with a span of 900 mm between supports and a constant a/d of 0.8. The beam was covered with a thin layer of clear concrete that was about 25 millimeters thick. Table 1 shows the names and descriptions of the sample.

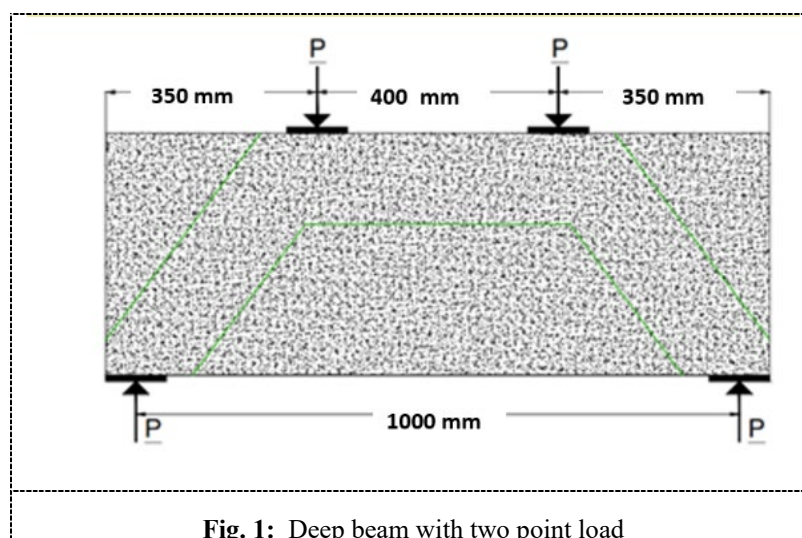
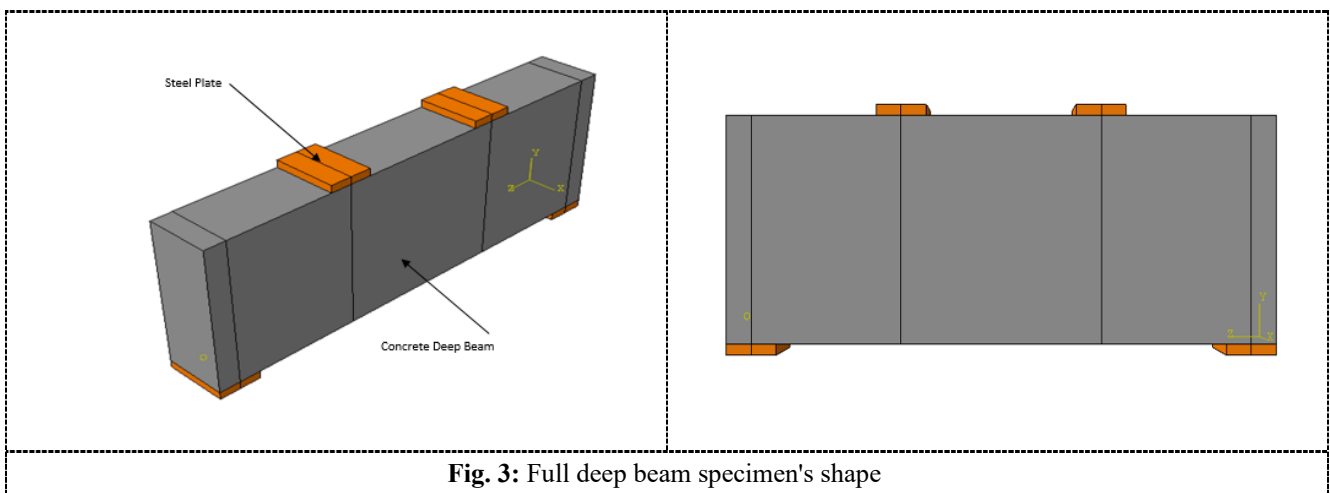
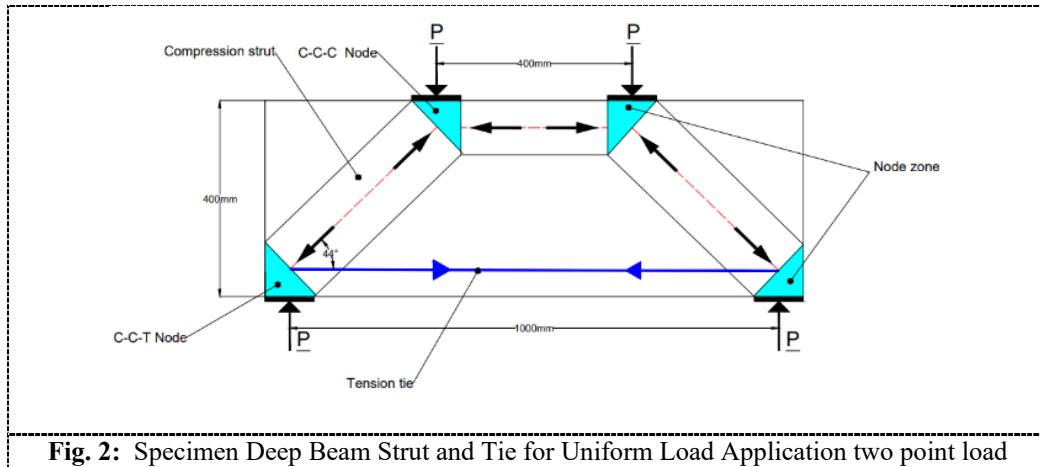


Table 1. Tested Deep Beam Specimens' names

No.	Specimens	Description
1	Sc	Reference deep beam specimen
2	S0a	0 percent of the surplus reinforcement from the web reinforcement was transferred to the reinforcement strut deep beam.
3	S0b	0 percent of the surplus reinforcement from the web reinforcement was transferred to the reinforcement strut deep beam.
4	S5	50 percent of the surplus reinforcement from the web reinforcement was transferred to the reinforcement strut deep beam.
5	S7.5a	75 percent of the surplus reinforcement from the web reinforcement was transferred to the reinforcement strut deep beam.
6	S7.5b	75 percent of the surplus reinforcement from the web reinforcement was transferred to the reinforcement strut deep beam.
7	S10	100 percent of the surplus reinforcement from the web reinforcement was transferred to the reinforcement strut deep beam.
8	S0.8	The deep strut beam employed a specimen with 80% reinforcement from the reinforced web.

2.2. The proposed strut and tie specimen

It is well knowledge that as beam depth increases, shear capacity decreases [2]. The shear behavior, represented by the diagonal compression strut, may thus be designed separately from the bending behavior of the DB. The suggested specimen was shown in figures 2 and 3. The concrete deep beam with reinforcement was represented as a truss, with the diagonal strut designed as an axially loaded compression column and the tension ties represented as flexural reinforcement, with the strut and ties linked at the nodes. (ACI-code318-14) To prevent the strut from collapsing under its own weight, the longitudinal compression reinforcement must run parallel to the strut's axis. A closed tie running the length of the strut is also necessary to prevent the strut from buckling diagonally under the stress of beam bending.



SC: Deep beam specimens with standard reinforcement underwent testing under two-point loading conditions, as shown in figure 4.

S0a: no surplus weight from the web reinforcement was employed. The load-distributed reinforcement includes vertical web reinforcement ($4\text{Ø}8\text{mm}$). Each diagonal strut features three rows of longitudinal reinforcement ($4\text{Ø}10\text{mm}$) and a closed tie ($10\text{Ø}100\text{mm}$), along with the main reinforcement ($4\text{Ø}16\text{mm}$), as illustrated in figure 5.

S0b: no surplus weight from the web reinforcement was employed, with load-distributed reinforcement featuring vertical web reinforcement ($4\text{Ø}8\text{mm}$). Each diagonal strut is equipped with three rows of longitudinal reinforcement ($4\text{Ø}10\text{mm}$), along with a closed tie ($13\text{Ø}10\text{mm}$) in the oblique strut and a tie ($1\text{Ø}10\text{mm}$) in the horizontal strut, in addition to the main reinforcement ($4\text{Ø}16\text{mm}$), as illustrated in figure 6.

S5: the 50% entirety of the surplus weight from the web reinforcement was employed. The load-distributed reinforcement includes ($1\text{Ø}10\text{mm}@250\text{mm}$) and ($4\text{Ø}8\text{mm}$) vertical web reinforcement. Additionally, each diagonal strut incorporates three rows of longitudinal reinforcement ($4\text{Ø}10\text{mm}$) and a closed tie ($10\text{Ø}100\text{mm}$), alongside the primary reinforcement ($4\text{Ø}16\text{mm}$), as illustrated in figure 7.

S75a: in this specimen, 75% of the surplus weight from the web reinforcement was employed for the three deep beams. The load-distributed reinforcement includes ($2\text{Ø}10\text{mm}@500\text{mm}$) and ($4\text{Ø}8\text{mm}$) vertical web reinforcement. Each diagonal strut is equipped with three rows of longitudinal reinforcement ($4\text{Ø}10\text{mm}$) and a closed tie ($10\text{Ø}100\text{mm}$), alongside the primary reinforcement ($4\text{Ø}16\text{mm}$), as illustrated in figure 8.

S75b: in this specimen, 50% of the surplus weight from the web reinforcement was employed. The load-distributed reinforcement includes ($2\text{Ø}10\text{mm}@500\text{mm}$) and ($4\text{Ø}8\text{mm}$) vertical web reinforcement. Furthermore, each diagonal strut is fitted with three rows of longitudinal reinforcement ($4\text{Ø}10\text{mm}$), along with a closed tie in the oblique strut ($21\text{Ø}10\text{mm}$) and in the horizontal strut ($1\text{Ø}10\text{mm}$), in addition to the primary reinforcement ($4\text{Ø}16\text{mm}$), as illustrated in figure 9.

S10: in this specimen, the entire surplus weight from the web reinforcement was employed. The load-distributed reinforcement encompasses ($3\text{Ø}10\text{mm}@250\text{mm}$) and ($4\text{Ø}8\text{mm}$) vertical web reinforcement. Moreover, each diagonal strut integrates three rows of longitudinal reinforcement ($4\text{Ø}10\text{mm}$), coupled with a closed tie ($10\text{Ø}100\text{mm}$), apart from the primary reinforcement ($4\text{Ø}16\text{mm}$), as illustrated in figure 10.

S0.8: all the surplus weight from the web reinforcement was utilized for the three deep beams in this set. The load-distributed reinforcement ($4\text{Ø}8\text{mm}$) vertical web reinforcement. Each diagonal strut has three rows of longitudinal reinforcement ($4\text{Ø}10$) and a closed tie in the $8\text{Ø}10\text{mm}$ oblique strut and in the $0\text{Ø}10\text{mm}$ horizontal strut in addition to the main reinforcement ($4\text{Ø}16$), as illustrated in figure 11.

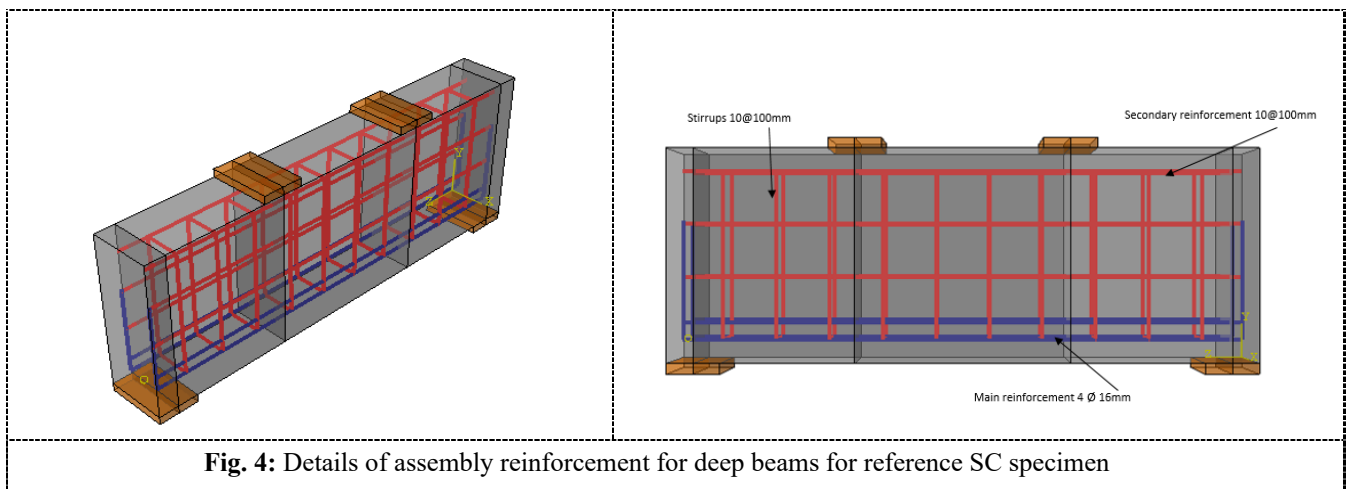


Fig. 4: Details of assembly reinforcement for deep beams for reference SC specimen

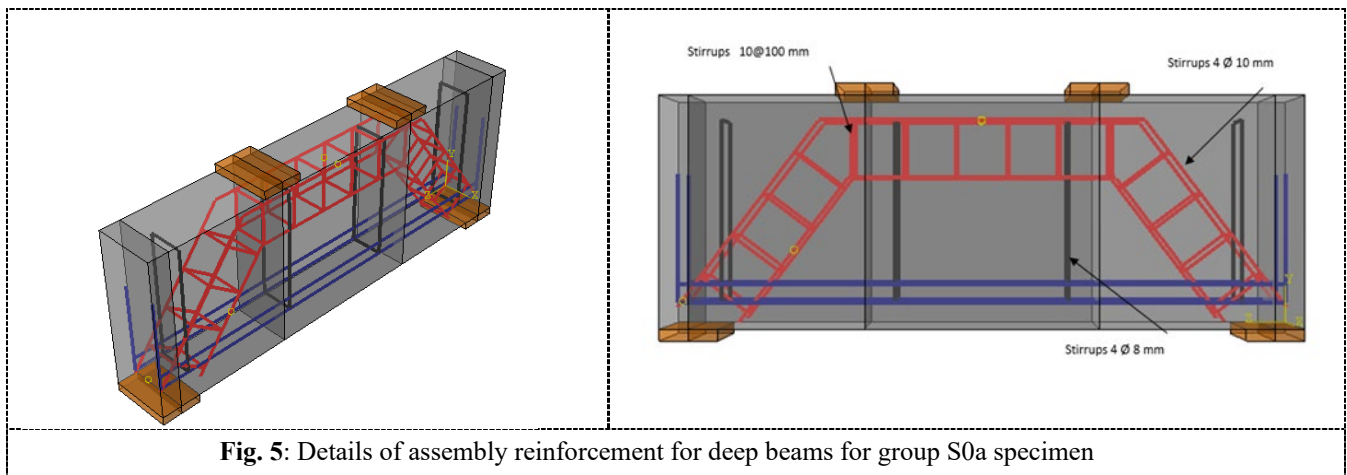


Fig. 5: Details of assembly reinforcement for deep beams for group S0a specimen

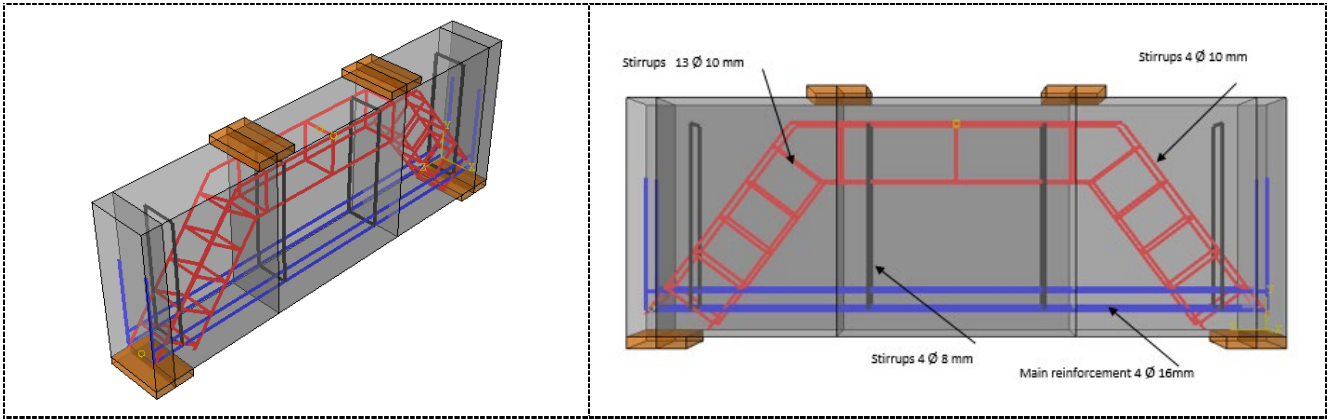


Fig. 6: Details of assembly reinforcement for deep beams for group S0b specimen

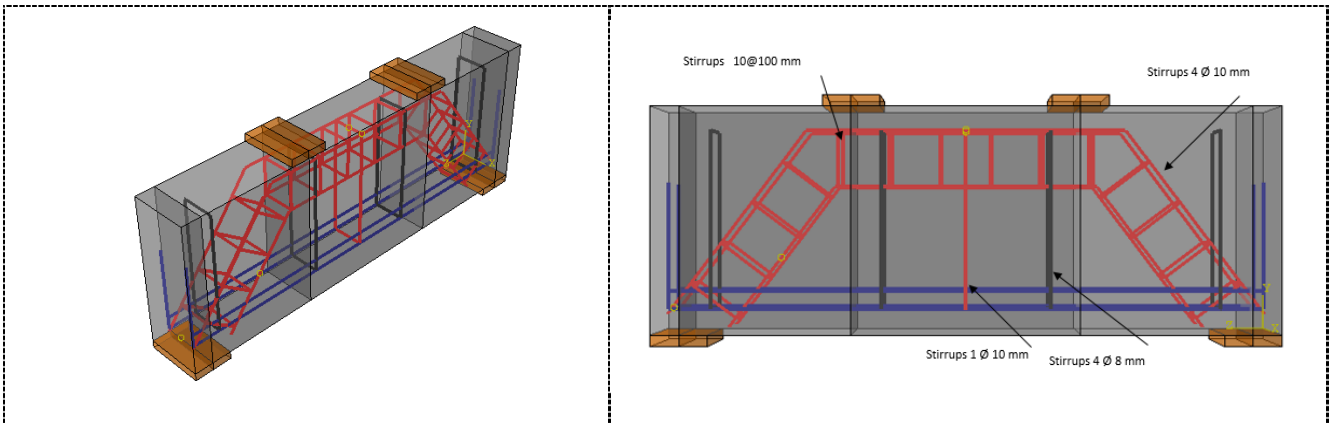


Fig. 7: Details of assembly reinforcement for deep beams for group S5 mode

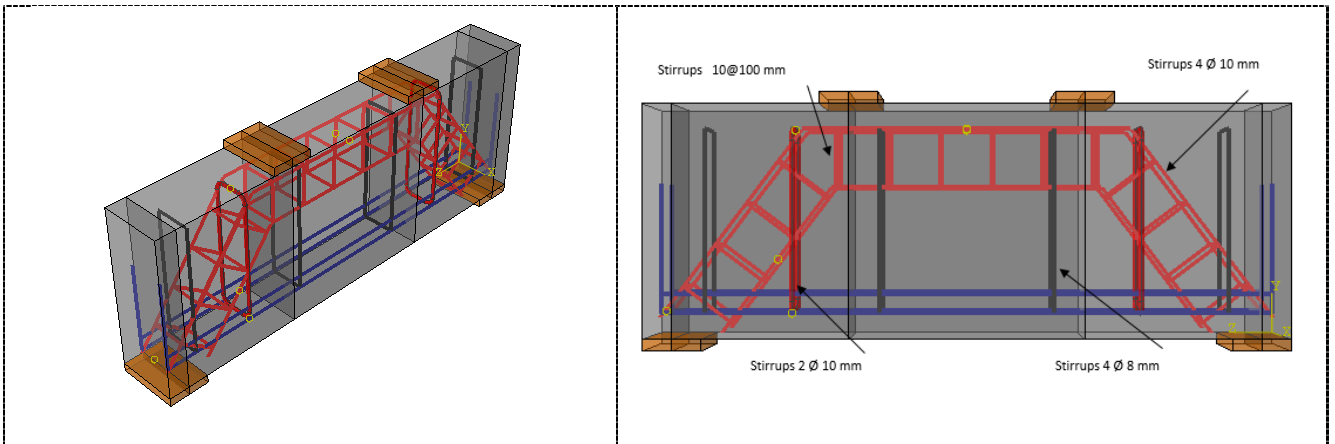


Fig. 8: Details of assembly reinforcement for deep beams for group S75a specimen

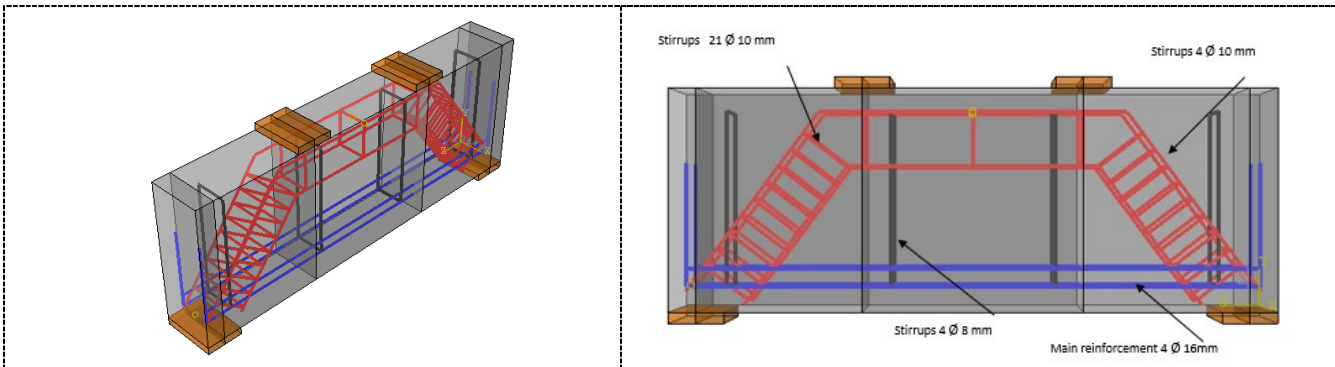


Fig. 9: Details of assembly reinforcement for deep beams for group S75b mod

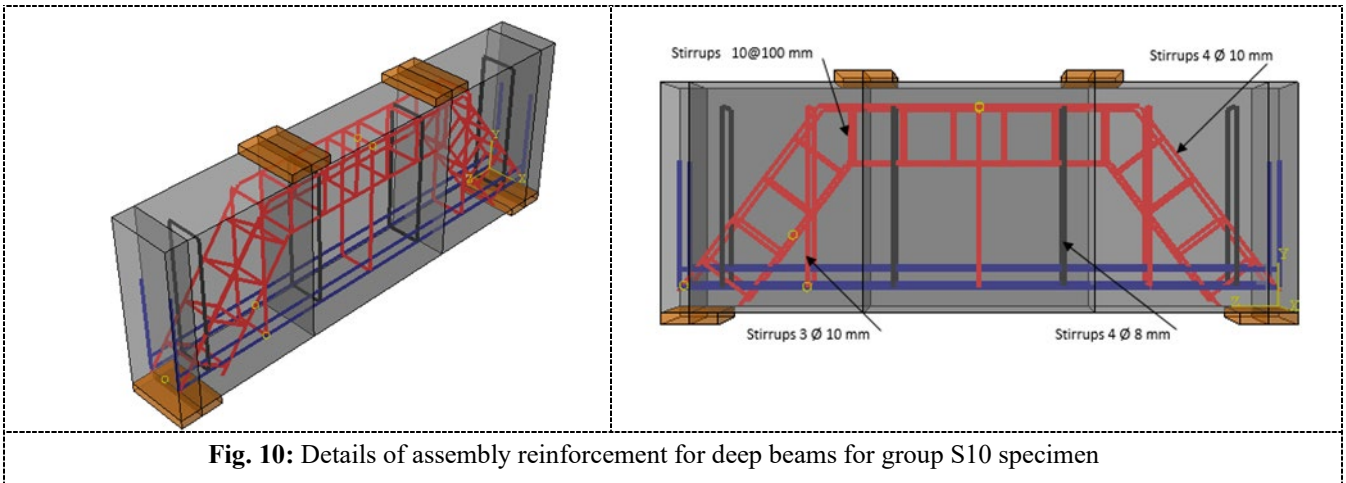


Fig. 10: Details of assembly reinforcement for deep beams for group S10 specimen

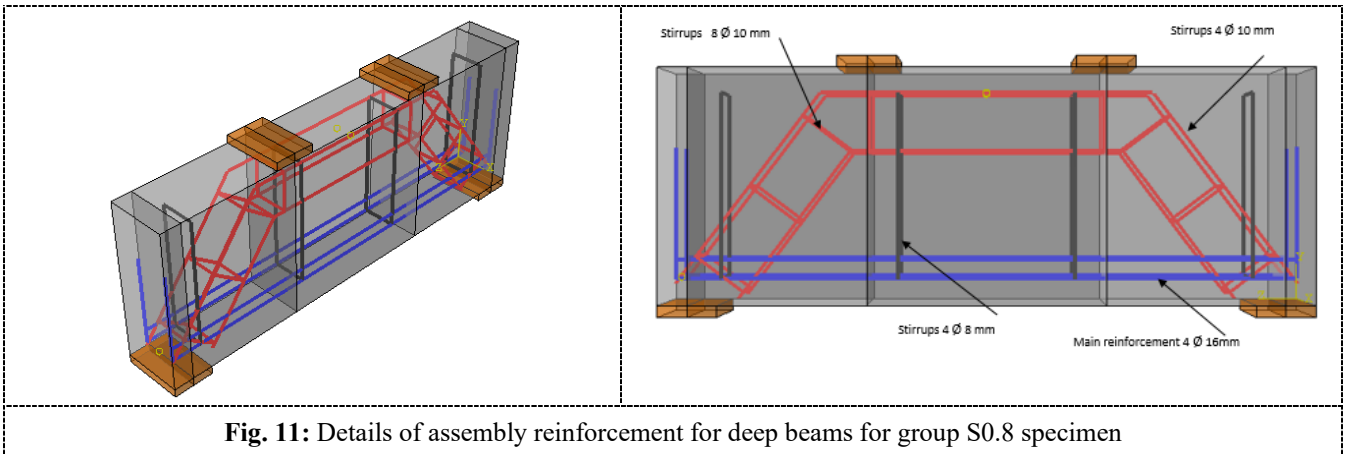


Fig. 11: Details of assembly reinforcement for deep beams for group S0.8 specimen

2.3. Testing specimens

In this Study, a total of each beam was specimen using three-dimensional solid elements as shown in figure 3. For the concrete, we utilized the eight-solid-element C3D8 illustrated in figures 4 to 11, and for the reinforcement we used the two-node truss element T3D2.

2.3.1. Description of finite element modelling

2.3.1.1. Mesh Refinement

Selecting the appropriate mesh density, as seen in figure 12 (a, b, c), is a crucial part of non-linear finite element modelling. When the right amount of elements are employed to build anything, the results start to converge. When an increase in mesh density has a minor effect on the outcomes, this goal effectively achieved. It has been observed that the higher the density of the mesh, the more visible the cracks and the more consistent the form of failure. Therefore, a proximity analysis was carried out in this finite element modelling to ascertain an appropriate mesh density. To examine the sensitivity of the FEM analysis and the mesh in all three dimensions, performed a convergence study by increasing the number of elements, as shown in figure 12. The effect of the deep beam (SC) on the mid span deflection was studied for three different types of mesh size (50, 30, and 15) under the same total applied load level. The specimen with a mesh size of 15 produces the best results.

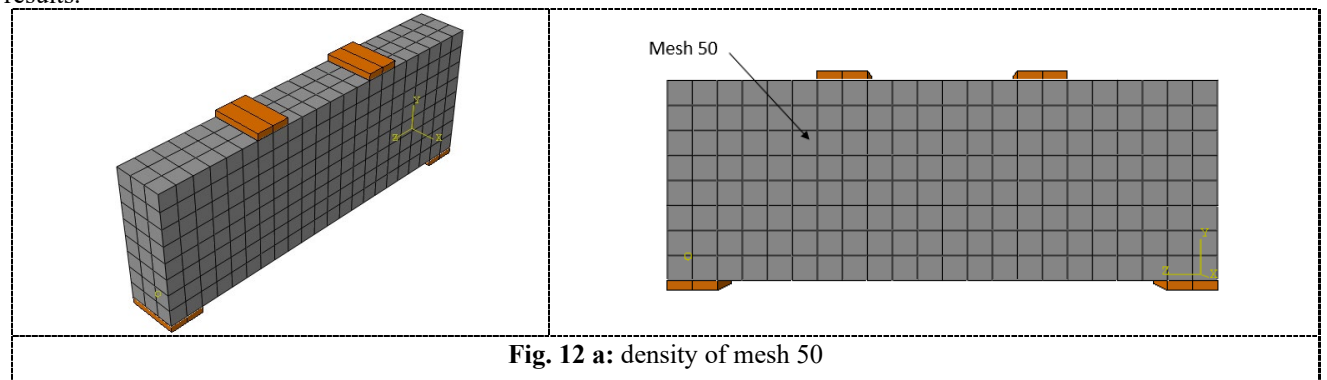
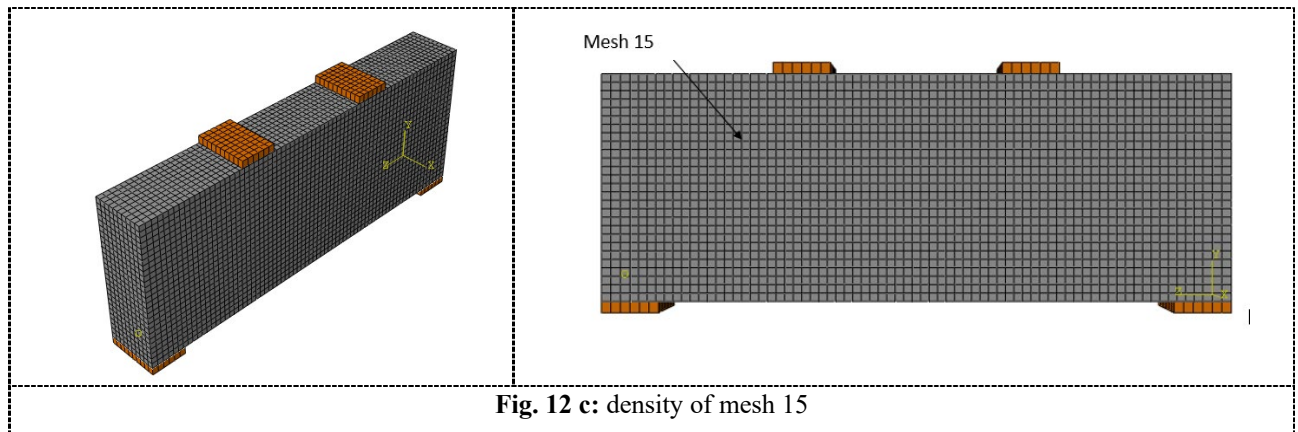
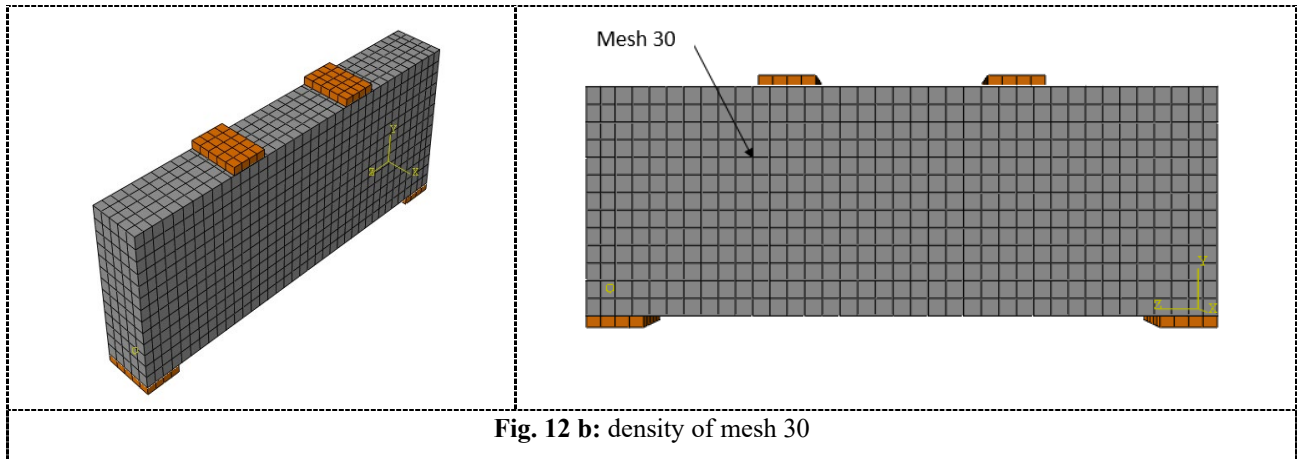
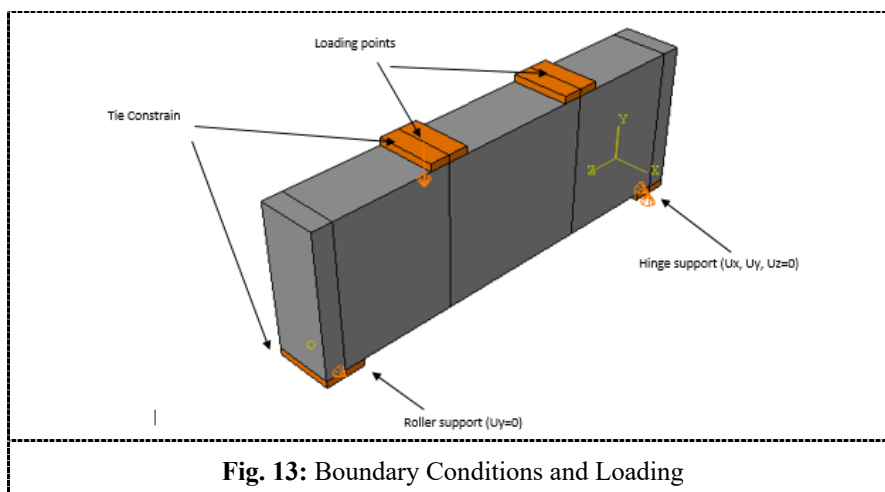


Fig. 12 a: density of mesh 50



2.3.1.2. Boundary Conditions and Loading

The pressure load was delivered as a uniform load by dividing the total load by the mesh elements for loading plate area (N/mm^2), and the load was shown by an area drawn in the top surface of the loading plate, the total load calculated by collect the load at each element from mesh load plate. The loading and support plates used in the experiment have dimensions of (150, 100, 10) mm and (150, 100, 10) mm, respectively. They were included into the specimen at the load and support bearing plate as a C3D8 solid element to counteract the potential for stress concentration there. The finite element specimen's loading and boundary conditions were shown in detail in figure 13.



Two-support plate boundary conditions were specified as follows:

- Support hinge: the node was fastened along the cross line in the center of the base plate, with its allowed range of motion limited to (y and x) in the z-axis.
- Roller's support: The node was placed at the cross line in the plate's bottom center, limiting its motion to only the y-axis

2.3.1.3. Interaction

ABAQUS provides a wide range of options for simulating communication between specimen components. These resources allow the specimen to converge to an accurate simulation of the experimental behavior of the examined specimens. The deep beam was connected to the loading and support plate by tie contact, which was employed without interaction to separate the plate and concrete surface, and embedding region constrain was used to link the steel reinforcement to the surrounding concrete (host beam). This indicates that the components will remain in place despite the force exerted. Check the Figures 14 a and b.

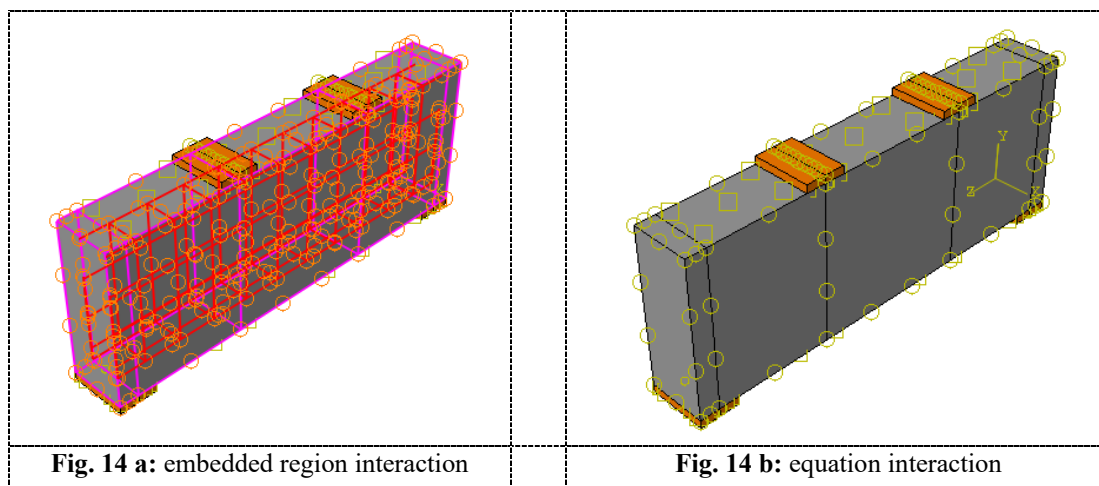


Fig. 14 a: embedded region interaction

Fig. 14 b: equation interaction

2.3.2. Finite element analysis

All members were analyzed experimentally under two point load to verify the validity and efficiency of the chosen finite element specimens using the ABAQUS computer programme.

2.3.3. Result for the specimens

The quantity of reinforcement and the maximum load for each specimen are in the table 2 below.

Table 2: Quantity of reinforcement and the maximum load for each specimen

ID	Reinforcement Quantity	Maximum Load
R	R	506.4
S0a	82.6	534.1
S0b	82.6	556.0
S5	88.4	536.0
S7.5a	94.2	540.7
S7.5b	94.2	558.0
S10	100	542.7
S0.8	-20	532.0

2.4. Discussing the outcomes of an experiment

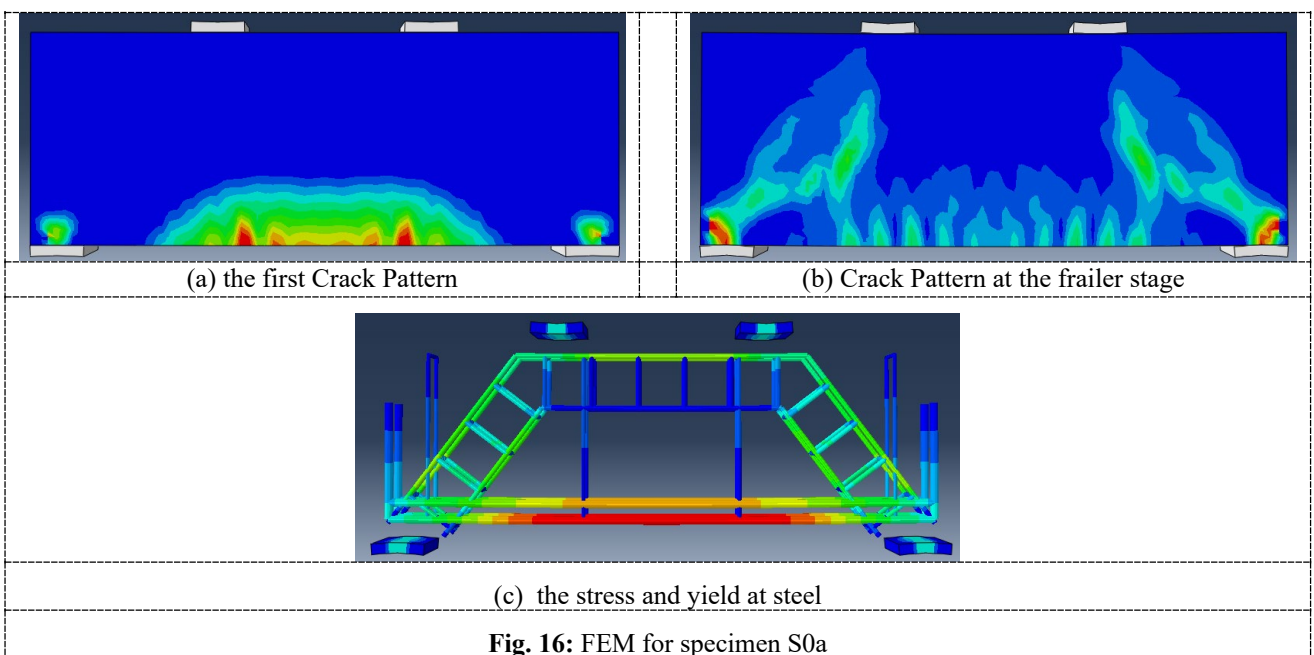
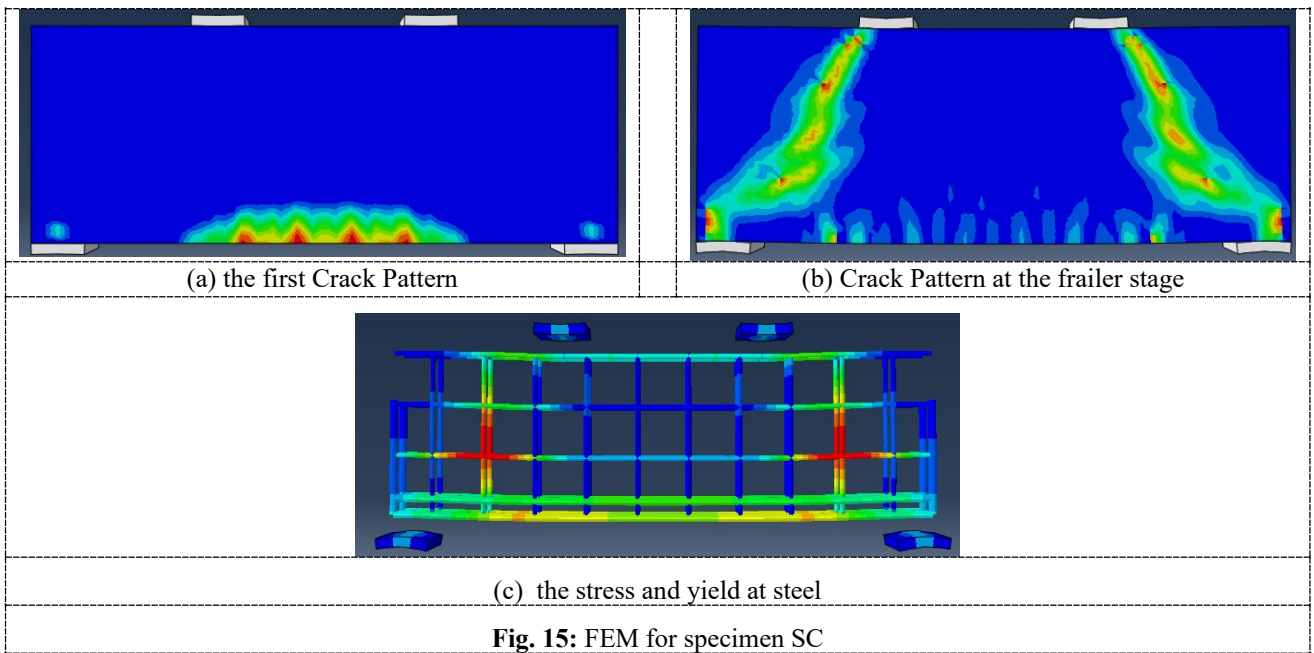
Crack patterns, easily recognizable failure modes, loads parallel and perpendicular to the strut axis, and ultimate capacity all be shown here as a consequence of the deep beam experimental testing system.

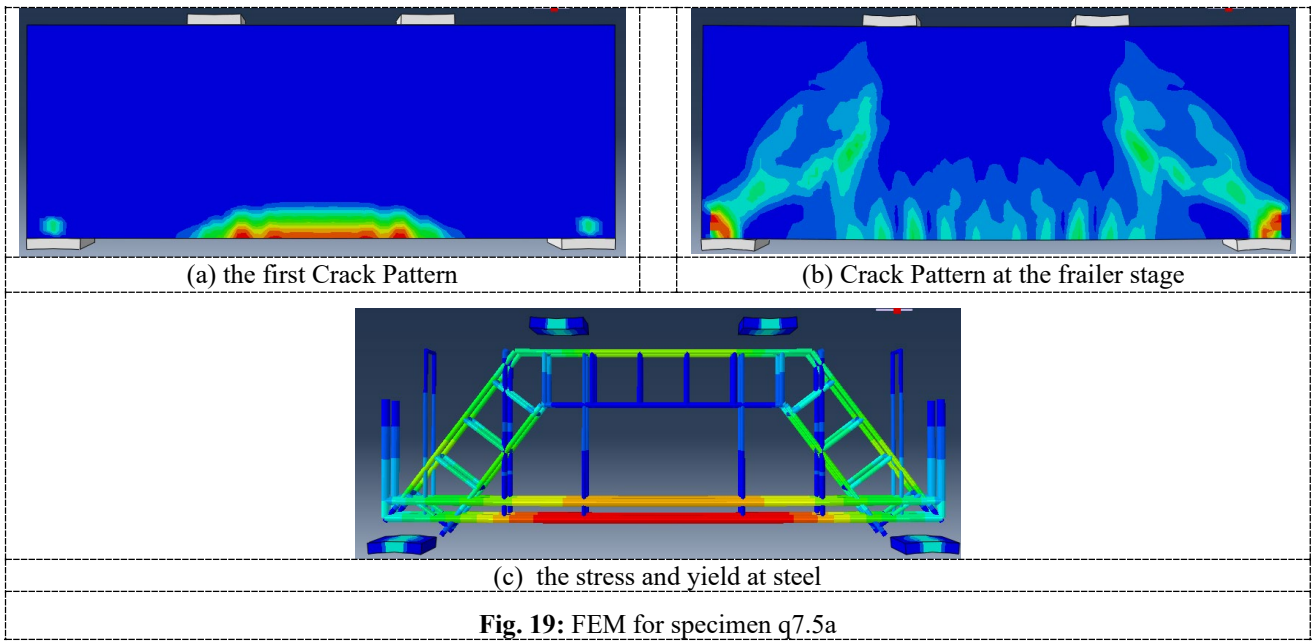
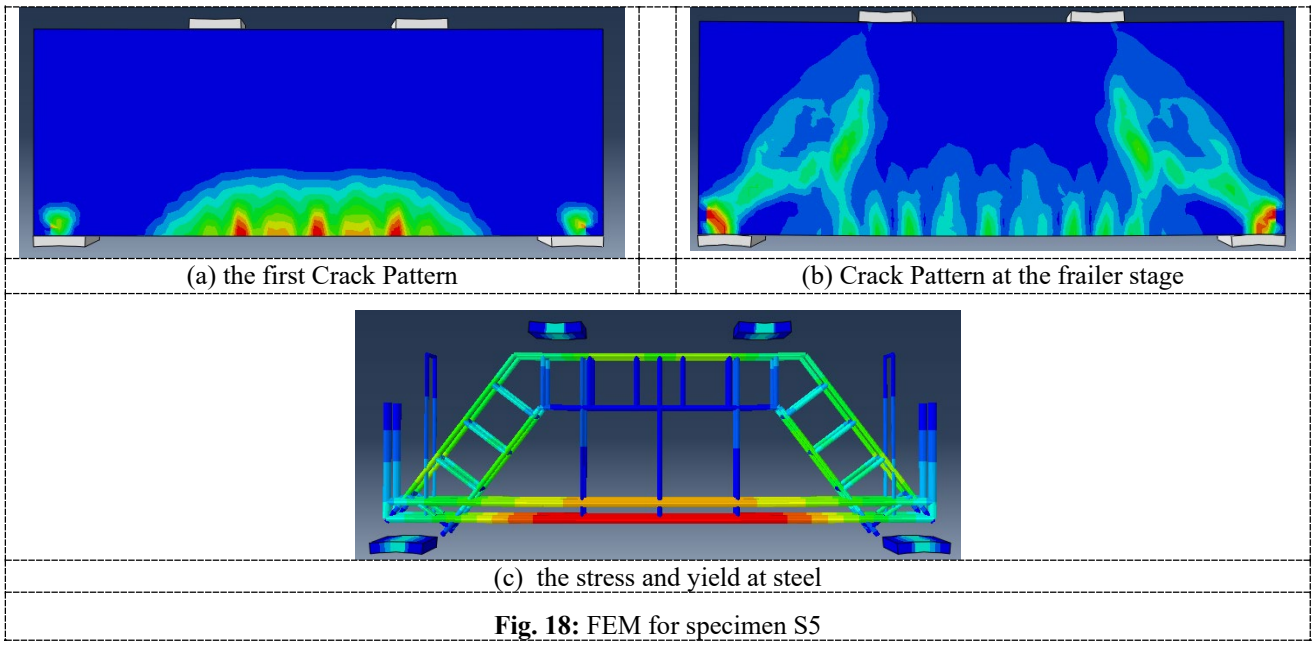
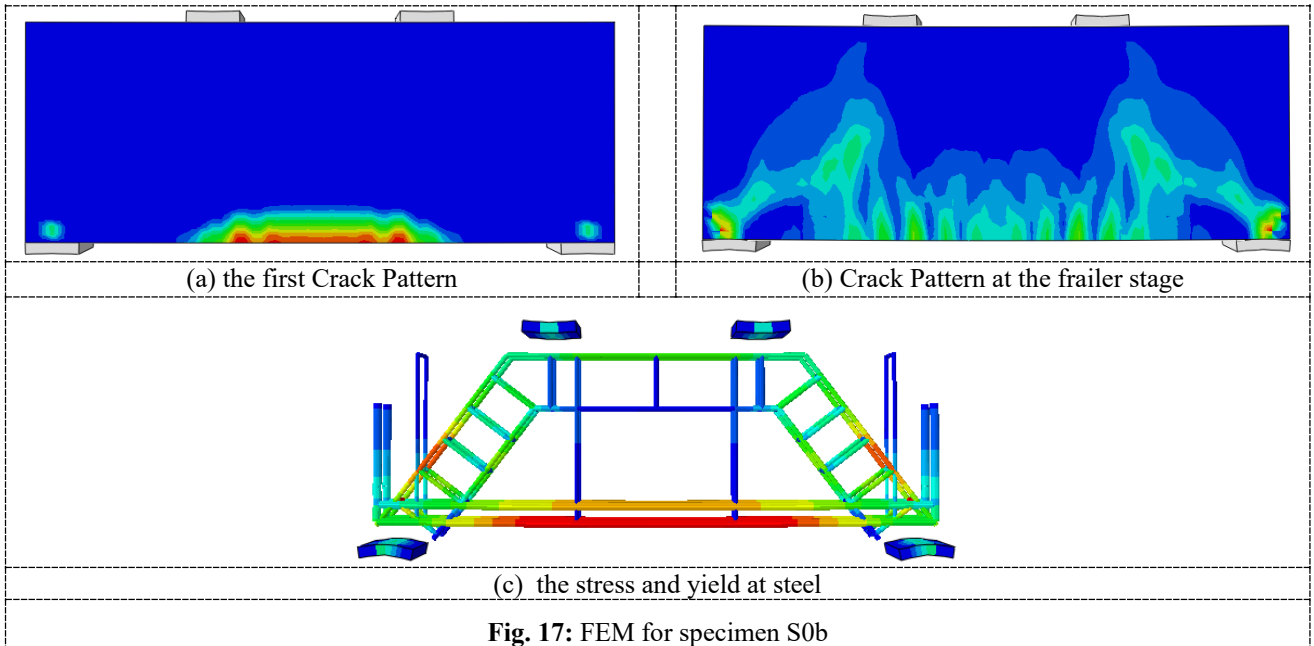
2.4.1. General behavior of deep beam

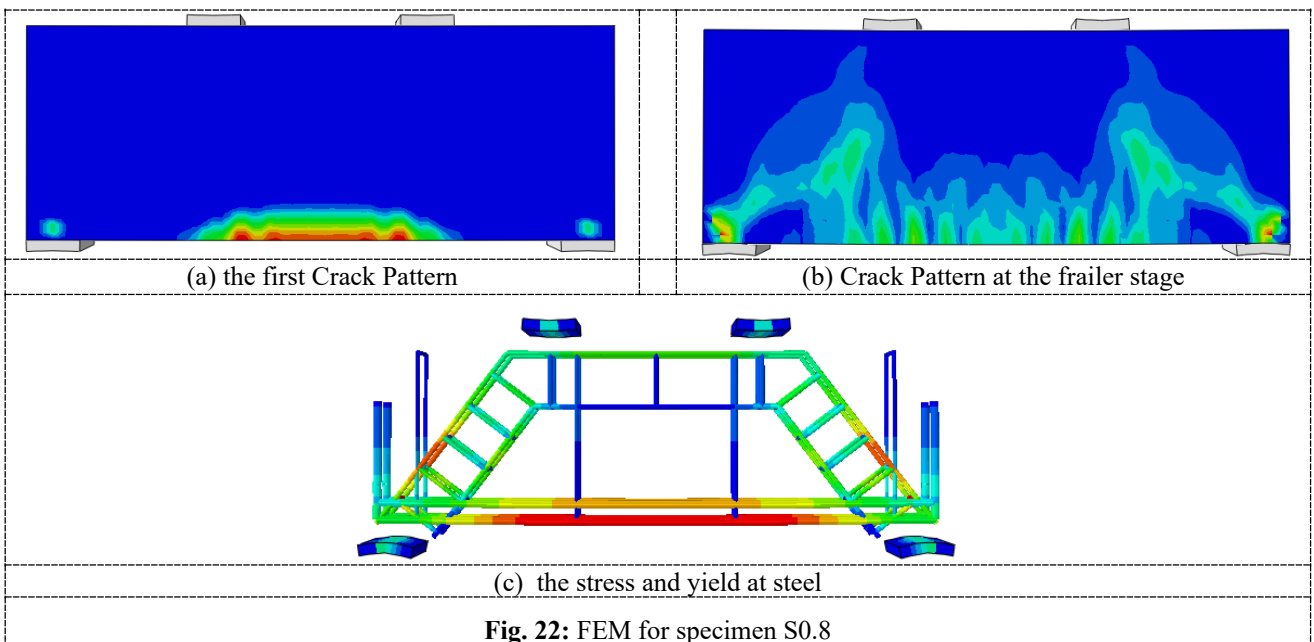
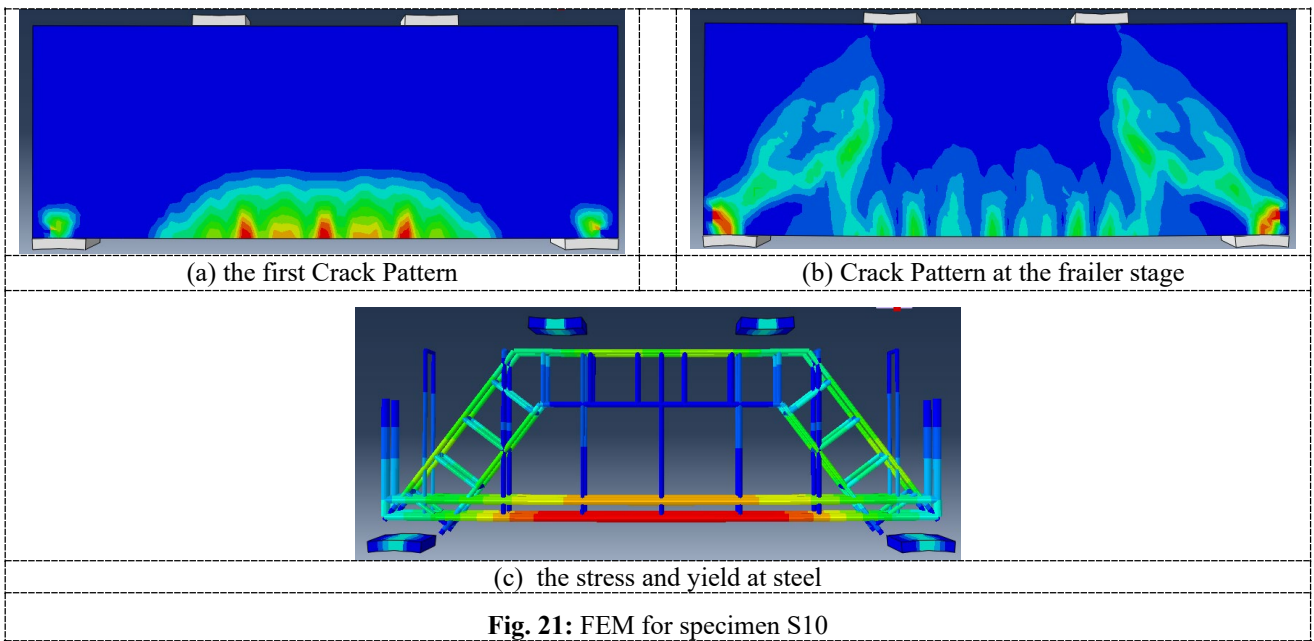
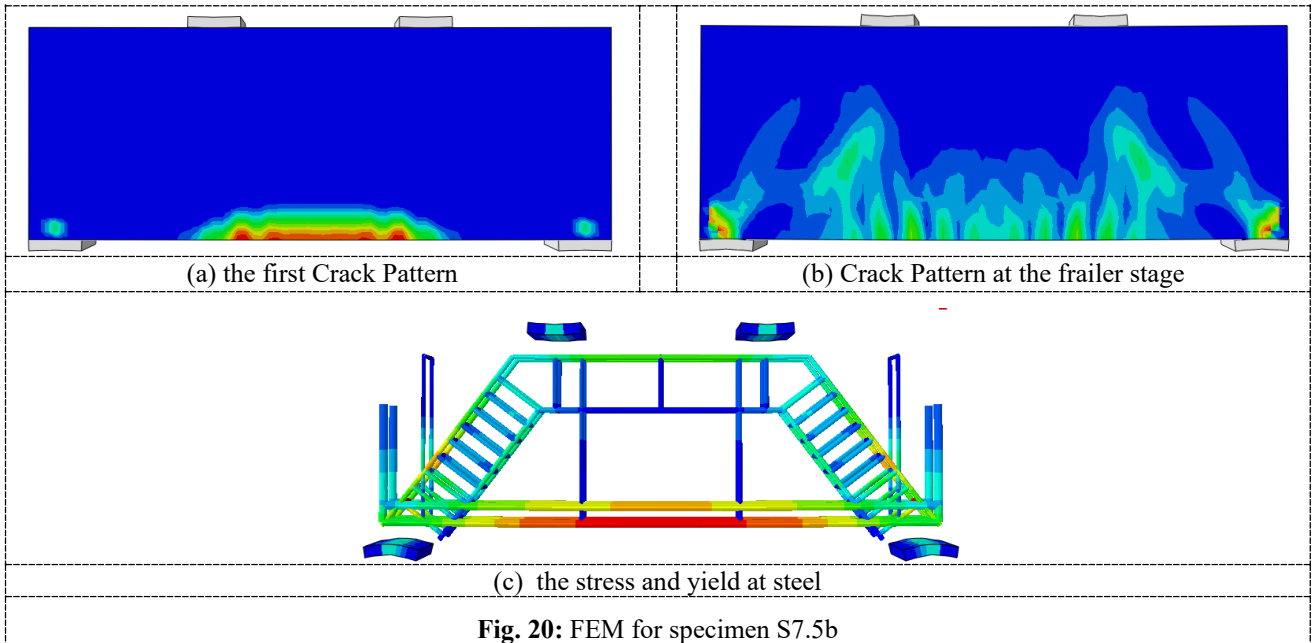
Two-point loads were applied to eight deep beam specimens. The deep beams exhibited elastic uncracked behavior both in the low load stage and under the applied stresses. As the load was raised, fractures emerged at the elastic cracked level of the deep beam, first in the flexural area and then in the shear span. The shear span area of the beams developed more fractures after this level. As the load was raised, the fracture appeared in the strut zone (shear span area), beginning at the middle depth of the beam shear span. The deep beam failed because the cracks began at the support plate and progressed towards the point of stress. The cracks widened and became larger in this area, which represents the shear area, which led to specimen failure.

2.4.2. Crack pattern

As depicted in figures 15 to 22 below and analyzed using the ABAQUS program, it is evident that during the initial phase of load increment, the cracks began to appear in the middle of the beam from the bottom and began to expand to the loading area, and after the loads increased, the cracks began to appear, and when the load increased, the inclined cracks began to grow and expand significantly and move from support to the loading area until failure Under two point load. The first crack in the specimens appeared at the mid distance between the supports. In further studies, it was shown that fractures emerge at the strut (shear span zones) and spread radially outward towards the point load. Once, crack reaches a critical size and the concrete collapses under shear, the deep beam has taken on as much weight as it can handle. Although this trend was seen in all test specimens, the specific kind of fracture that developed in each specimen varied according to the reinforcing details. In the strut failure crushing, there are more than one inclined crack. The inclined cracks concrete was compression parts. After the formation of the inclined crack, the concrete part above the upper end of this crack exposed high compression and the concrete above the crack failed by crushing with high noise. Compression forces from the load caused the strut to fail. A large amount of noise was produced as a consequence of the strut's failure mode, which was characterized by cracking and crushing.







2.5. Discussion

2.5.1. Maximum load capacity and reinforcement percent

The percentage of reinforcement and load maximum capacity was shown in the table 3 below, where the specimen of S0.8 was the lowest reinforcement ratio among the specimens and the specimen of S7.5 b was the highest load maximum capacity.

Table 3: Maximum load with reinforcement percent

ID	Reinforcement	Maximum	Reinforcement %	Load Capacity %
	Quantity	Load		
R	100	506.4	0	0
S0a	82.6	534.1	17%	105%
S0b	82.6	556	17%	110%
S5	88.4	536	12%	106%
S7.5a	94.2	540.7	6%	107%
S7.5b	94.2	558	6%	110%
S10	100	542.7	0%	107%
S0.8	-20	532	42%	105%

2.5.2. Load Displacement Curve

All specimens showed a similar progression. There were three stages: elasticity without cracks and elasticity with cracks, and the third one the plasticity stage. At the first stage after the load is removed, the specimen goes back to its original form without any changes. At the second stage, cracks emerge and the specimen is elastic enough to recover to its previous shape but with cracks. The third stage at this point, the specimen has already failed and can no longer be restored to its former state. The smallest displacement was found in the S7.5b specimen (2.14 mm), with the largest displacement (5.15 mm) found in the SC specimen. See the data in figures 23 to 30.

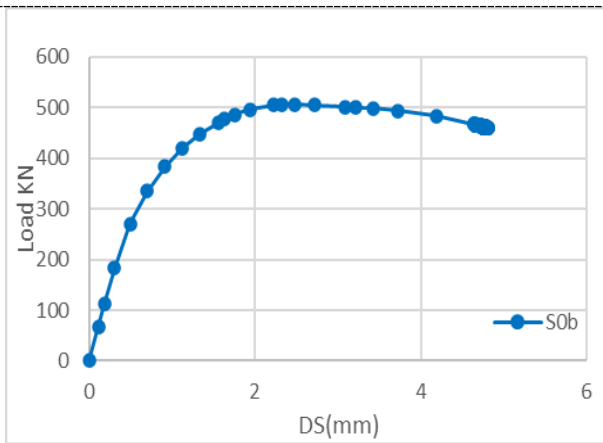


Fig. 23: Load Displacement curve for SC

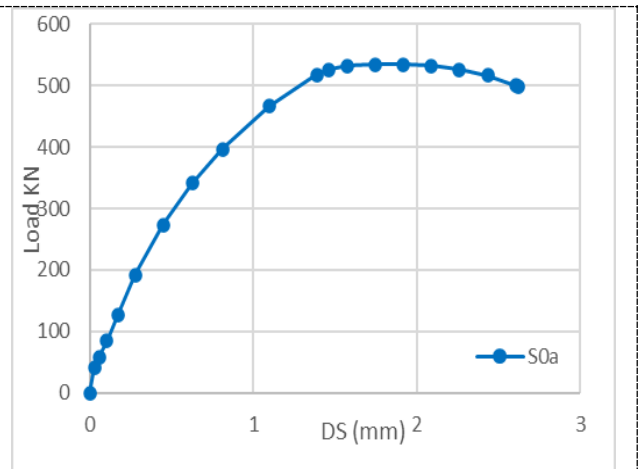


Fig. 24: Load Displacement curve for S0a

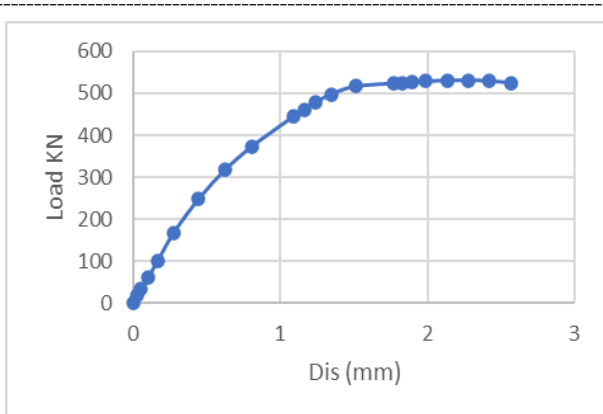


Fig. 25: Load Displacement curve for S0b

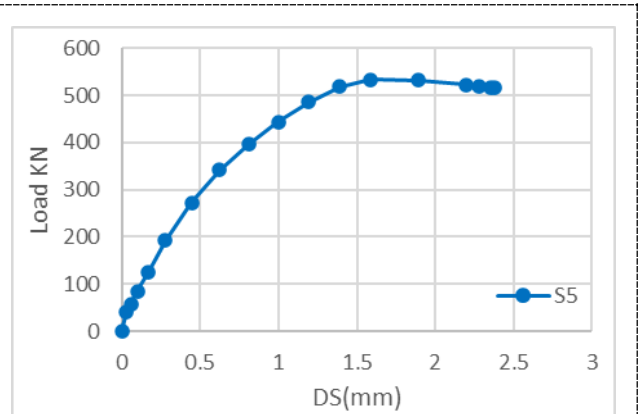


Fig. 26: Load Displacement curve for S5

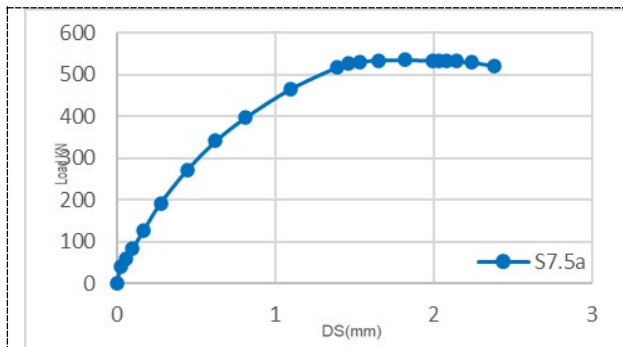


Fig. 27: Load Displacement curve for S7.5a

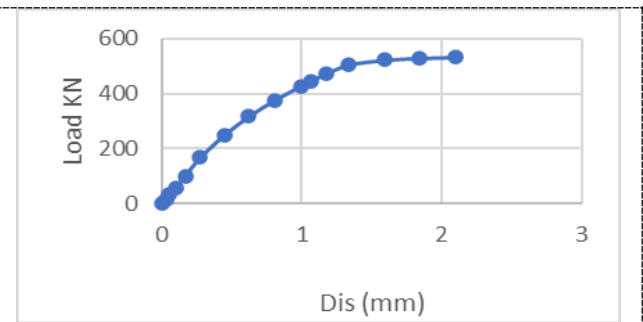


Fig. 28: Load Displacement curve for S7.5b

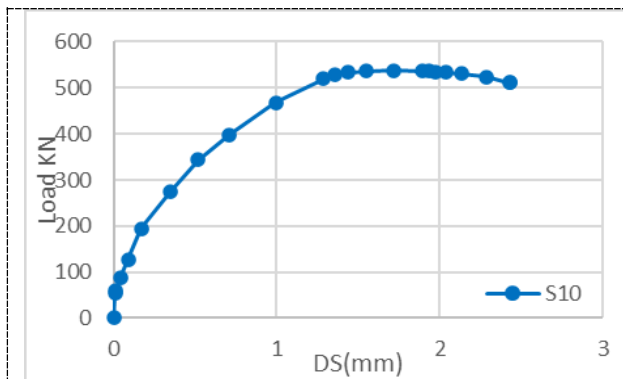


Fig. 29: Load Displacement curve for S10

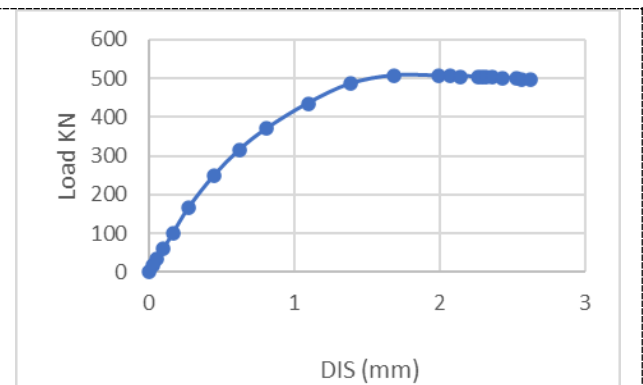


Fig. 30: Load Displacement curve for S0.8

3. Conclusions

Through this research, it was found that the reinforcement of the strut area was more efficient than the normal reinforcement, where the resistance of the specimens increased by 10% with a reduction in the percentage of reinforcement in the compression zone by 17% in the S0b specimen or increased by 5% with a decrease in the amount of reinforcement in the compression area by 42% in the S0.8 specimen. It was also noted that the reinforcement in the horizontal strut area is not of great importance and does not affect the maximum resistance beam, and the increase in the reinforcement in the inclined strut area was directly affected with the maximum resistance as well as reducing the displacement. The study also revealed that having additional reinforcement, such as shear reinforcement or any other reinforcement, in the mid-span of a deep beam and away from the stress zone does not provide any significant benefit, unlike reinforcement in the stress zone, which increases the strength of the beam. It was also noted that cracks are formed in the shear and flexural zones at reference specimen when a load less than the specimens with strut is applied. The displacement in specimens with strut was less than of reference sample. It was also found that strain in specimens with strut reinforcement was lower than in reference sample.

References

- [1] Cheng, J. J. R., & Tan, K. H. (2006). Shear strength of deep beams. *Journal of Structural Engineering*, 132(12), 1979-1989.
- [2] Oh, J. K., & Shin, S. W. (2001). Ultimate shear and symmetric diagonal cracking strengths of high-strength concrete deep beams. *ACI Structural Journal*, 98(2), 157-166.
- [3] Lu, W.-Y., Zhou, Y.-Q., Yu, Y.-S., Zhang, G.-H., & Song, Q.-W. (2013). Shear Strength of Reinforced Concrete Deep Beams: Experimental Study and Analytical Specimens. *Journal of Structural Engineering*, 139(11), 1891-1902.
- [4] ACI (American Concrete Institute). "ACI 318-08 Strength Theory Specimen (STM)," 2008.
- [5] Ismail, K. S. (2016). Experimental and Numerical Investigation of Reinforced Concrete Deep Beams. *International Journal of Civil, Environmental, Structural, Construction and Architectural Engineering*, 10(2), 207-214.
- [6] Khattab Saleem Abdul-Razzaq, H., et al. (2018). Implementation of the Strut and Tie Method for Noncentral Loadings on Reinforced Concrete Deep Beams. *Journal of Materials in Civil Engineering*, 30(5), 04018040.
- [7] Haider K. Ammash1* and Maryam M. AL-Mousawi. (2021). Experimental Investigation of Deep Beam Reinforced with Different Types of Reinforcement. *Engineering, Technology & Applied Science Research*, 11(2), 7585-7590.
- [8] Ing Zhang, Kang-Hai Tan. (2007). Size effect on shear strength of deep beams. *Journal of Structural Engineering*, 133(3), 368-378.
- [9] Ismail, K. S. (2016). Experimental and Numerical Investigation of Reinforced Concrete Deep Beams. *International Journal of Civil, Environmental, Structural, Construction and Architectural Engineering*, 10(2), 207-214.

- [10] Kondalraj, R., & Appa Rao, G. (2021). Experimental Evaluation of Deep Beams with Web Reinforcement. *International Journal of Concrete Structures and Materials*, 15(1), 9.
- [11] Mona Saleha Mohammad Al-Hamaydeh, Mohamed Zakariac (2023). Behavior of Reinforced Concrete Deep Beams with Web Apertures. *Construction and Building Materials*, 314, 125971.
- [12] R Kondalraj, G Appa Rao. (2022). Experimental Evaluation of Strut Efficiency Factors for Reinforced Concrete Deep Beams. *International Journal of Concrete Structures and Materials*, 16(1), 1-12.
- [13] Smith, J., & Johnson, R. (2023). "Investigation of the Behavior of Simply Supported Reinforced Concrete Deep Beams under Concentrated Point Loading." *Journal of Structural Engineering*, 146(5), 04020128.
- [14] Chen, Z., & Wang, Y. (2023). "Performance Evaluation of Normal Strength Reinforced Concrete Deep Beams under Triangular Distributed Loading." *Journal of Structural Engineering*, 146(9), 04020140
- [15] Zhang, L., & Liu, H. (2023). "Behavior of Reinforced Concrete Deep Beams under Combined Loading." *Journal of Structural Engineering*, 146(10), 04020162.
- [16] ACI (American Concrete Institute). Code 318-14. Chapter 23 - Strut and Tie Specimens.